Journal of Hydrology: Regional Studies 13 (2017) 43–57

Contents lists available at ScienceDirect

Journal of Hydrology: Regional Studies

journal homepage: www.elsevier.com/locate/ejrh

Quantifying the effects of wildfire on changes in soil properties by surface burning of soils from the Boulder Creek Critical Zone Observatory

Celeste Wieting[a], Brian A. Ebel[b], Kamini Singha[a,c,*]

[a] Hydrologic Science and Engineering Program, Colorado School of Mines, 1500 Illinois St., Golden, CO 80401, USA
[b] U.S. Geological Survey, National Research Program, Kipling St, Lakewood, CO 80225, USA
[c] Geology and Geological Engineering Program, Colorado School of Mines, 1500 Illinois St., Golden, CO 80401, USA

ARTICLE INFO

Keywords:
Wildfire
Soil core
Bulk density
Hydraulic conductivity
Infiltration
Boulder creek critical zone observatory

ABSTRACT

Study region: This study used intact soil cores collected at the Boulder Creek Critical Zone Observatory near Boulder, Colorado, USA to explore fire impacts on soil properties.

Study focus: Three soil scenarios were considered: unburned control soils, and low- and high-temperature burned soils. We explored simulated fire impacts on field-saturated hydraulic conductivity, dry bulk density, total organic carbon, and infiltration processes during rainfall simulations.

New hydrological insights for the region: Soils burned to high temperatures became more homogeneous with depth with respect to total organic carbon and bulk density, suggesting reductions in near-surface porosity. Organic matter decreased significantly with increasing soil temperature. Tension infiltration experiments suggested a decrease in infiltration rates from unburned to low-temperature burned soils, and an increase in infiltration rates in high-temperature burned soils. Non-parametric statistical tests showed that field-saturated hydraulic conductivity similarly decreased from unburned to low-temperature burned soils, and then increased with high-temperature burned soils. We interpret these changes result from the combustion of surface and near-surface organic materials, enabling water to infiltrate directly into soil instead of being stored in the litter and duff layer at the surface. Together, these results indicate that fire-induced changes in soil properties from low temperatures were not as drastic as high temperatures, but that reductions in surface soil water repellency in high temperatures may increase infiltration relative to low temperatures.

1. Introduction

Wildfires often lead to enhanced runoff generation in mountainous environments. The Colorado Front Range in the US has experienced flash floods (e.g., Moody and Martin, 2001; Kunze and Stednick, 2006; Kinoshita et al., 2016), erosion (Benavides-Solorio and MacDonald, 2001, 2005; Wagenbrenner et al., 2006; Kampf et al., 2016) and water-quality problems (e.g., Murphy et al., 2015; Mast et al., 2016) following wildfire. Post-fire changes in soil-physical and soil-hydraulic properties are important for controlling the magnitude of the hydrologic response to rainfall. Physical properties of interest include organic matter, bulk density (ρ_d), and the strength and persistence of soil-water repellency. Changes in these physical properties are linked with effects on soil-

* Corresponding author at: Hydrologic Science and Engineering Program, Colorado School of Mines, 1500 Illinois St., Golden, CO, 80401, USA.
E-mail address: ksingha@mines.edu (K. Singha).

http://dx.doi.org/10.1016/j.ejrh.2017.07.006
Received 5 April 2017; Received in revised form 27 July 2017; Accepted 28 July 2017

hydraulic properties of field-saturated hydraulic conductivity, K_{fs}, and sorptivity of water, S_w, which directly impact infiltration and runoff generation.

Prior work in the Colorado Front Range has shown that wildfire affects soil-physical and soil-hydraulic properties. For example, based on field measurements and soil sampling in fire-affected areas, soil-organic matter often decreases after surface heating by wildfire (e.g. Ebel, 2012; Moody and Ebel, 2012), ρ_d increases (Moody and Martin, 2001; Moody et al., 2009; Ebel, 2012; Moody and Ebel, 2012), the strength and persistence of soil-water repellency can be increased (e.g. Huffman et al., 2001; MacDonald and Huffman, 2004; Lewis et al., 2006), and soil-hydraulic properties K_{fs} and S_w typically decrease in magnitude (e.g. Moody and Ebel, 2012; Ebel et al., 2012, 2016; Moody et al., 2016). The aforementioned research has led the way in addressing fire effects on soil-physical and hydraulic properties in the Colorado Front Range for individual properties or several properties in combination, but these studies have not integrated all these soil properties at the same site to further elucidate linkages and dependencies.

Wildfire impacts can depend on burn severity. The definition of burn severity from Keeley (2009), applied to the soil system, refers directly to the loss of organic matter driven by soil heating. The Colorado Front Range has historical wildfire regimes of low and high-severity (e.g. Veblen and Lorenz, 1986) and magnitudes of soil property changes in this region have been shown to depend on remotely sensed burn-severity metrics (Lewis et al., 2006; Moody et al., 2016). Currently we lack systematic understanding of the impact of burn severity on soil-physical and hydraulic property changes that is applicable across multiple soil types and fire regimes (Moody et al., 2016). Field measurements campaigns examining this issue (e.g. Moody et al., 2016) have proven instructive, but experimental burning of soils in the laboratory to simulate different wildfire severities offers another way forward.

The most controlled way to evaluate and quantify changes in physical properties of soils as a result of fire effects is through laboratory experiments. Prior work on experimental soil heating investigating soil property changes as a function of burn severity typically used repacked soil samples in laboratory experiments that do not represent intact soils. Previous laboratory studies have tried to simulate the effects of wildfires on soils through different heating or burning methods, observing changes in properties—such as field-saturated hydraulic conductivity, water repellency, and soil moisture— and processes, such as infiltration (e.g. Badía and Martí, 2003a; Doerr et al., 2004; Stoof et al., 2010). However, finding a realistic way to simulate fire effects on a soil core is challenging. Stoof et al. (2010) found that heating soils in a muffle furnace to 300 °C and above for 30 min can result in similar soil physical effects as burning the soil for 5 min with a propane burner. However, several laboratory studies have shown that heating soils in a muffle furnace does not address the movement of hydrophobic substances into the soil profile, and clearly does not allow for the direct effect of the flames on the soil (Badía and Martí, 2003b; Doerr et al., 2004; Glass et al., 2008; Stoof et al., 2010). Most laboratory studies on fire-impacted soils have also used sieved or disturbed soils (e.g. Forgeard and Frenot, 1996; Fernández et al., 1997; Moody et al., 2009; Stoof et al., 2010; Hatten and Zabowski, 2010; Bodí et al., 2012). However, it is unclear how well these results would mimic expected changes in properties in the field, as repacked soils rarely represent realistic water movement through structured field soils. One notable exception is the study by Cancelo-González et al. (2012); they heated intact cores by surface warming with infrared lamps to simulate fire effects, but focused on soil cations rather than physical and hydrologic impacts. The work by Gabet (2014) in chaparral areas of California in the US is another example of direct surface heating of intact samples, but is not similar to vegetation communities or soil types in the Colorado Front Range and this study focused on wind erosion. An additional challenge is assessing soil burn severity during a heating experiment to reach target burn severity values because it is not possible to measure soil organic matter loss during heating.

The primary objectives of this work were to investigate soil-physical and hydraulic properties as a function of soil burn temperature and duration using intact core samples from the field. Soil temperatures during burning were monitored to assess soil conditions, thus soil temperature/duration conditions are used herein as a surrogate for soil burn severity. We examined an area in the Colorado Front Range, where wildfires cause flash flooding and water quality issues (e.g., Morris and Moses, 1987; Murphy et al., 2015), that has not had systematic examination of burn severity controls on soil-physical and hydraulic properties in a controlled laboratory experiment. We seek to address the following research questions:

1. Do the magnitudes of soil-physical and hydraulic properties change monotonically with increasing burn temperature?
2. Are the trends between soil-physical and hydraulic properties as a function of soil burning similar?
3. What are the implications of measured trends in soil-physical and hydraulic properties as a function of soil burning for runoff generation in the wildfire-prone region of the Colorado Front Range?

2. Methods

Soil cores from the Boulder Creek Critical Zone Observatory in Colorado, USA (Fig. 1) were used in controlled surface burning experiments to quantify soil property and hydrologic process changes in cores at different two soil burning temperatures (low and high temperature, and a control, unburned case), defined by soil temperatures and duration of exposure (Certini, 2005). Our experiments simulated wildfire using a heat gun followed by rainfall simulation. This work explores relations between different temperatures of soil burning and physical soil properties, soil hydraulic properties, infiltration, and drainage following simulated rainfall. Our measurements include 1) dry bulk density, ρ_d, and loss on ignition (LOI) as a metric of total organic carbon (TOC), which provide insight into soil-water storage; 2) volumetric soil moisture; 3) water repellency persistence using both water drop penetration times (WDPT) and tension infiltration measurements; 4) field-saturated hydraulic conductivity, K_{fs}, used because air entrapment and water repellency prevent full soil saturation under field conditions (Reynolds et al., 1983); and 5) drainage of cores following simulated rainfall.

Eighteen soil samples were collected in the field within sections of polyvinyl chloride (PVC) pipe measuring 10 cm in height and

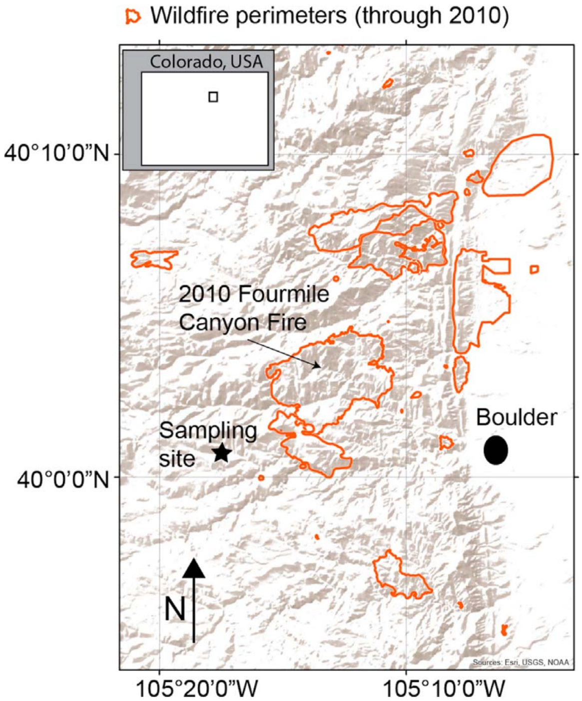

Fig. 1. Map showing the location of the soil sampling site at the Boulder Creek Critical Zone Observatory near Boulder, Colorado, and recent wildfire perimeters in the Colorado Front Range.

20 cm in diameter. When collecting the field cores, the inside of the core tube was coated in petroleum jelly to prevent a pathway for water to run down along the interface of the soil and PVC pipe. Three scenarios were considered with these cores, where six were unburned, six were burned to low temperatures, and six were burned to high temperatures; the process of simulated burning is described below. Half of the samples were used for tension infiltrometer testing and destructive sampling, the other half were used in the WDPT tests and rainfall simulations. Three replicates were considered for each unburned, low-temperature burned, and high-temperature burned scenario in each treatment to help quantify variability. The small sample sizes are a function of the difficulty of removing large diameter (i.e. 20 cm) intact soil cores from a mountainous area with stones and small roots embedded in the soil profile. Details on all procedures are below and a summary of methods is shown in Table 1.

2.1. Soil sample collection

Undisturbed soil samples were collected in the Boulder Creek Critical Zone Observatory outside Boulder, Colorado, USA. A low-lying area of approximately 50 m^2 on the north-facing slope near Lower Gordon Gulch Creek (40.011976, −105.462776) served as the sample location due to ease of access, lack of large trees, and flat slope, which enhanced undisturbed core removal. Soil cores were collected from 0 to 10 cm depth using PVC pipe that was hammered into the ground; a large hole was then dug around the PVC pipe to carefully slide sheet metal under it for removal. The soils are characterized as aquic arguidolls that vary in composition with depth (NRCS Soil Survey, 2017).

2.2. Wildfire simulation by laboratory burning

The soil-temperature treatments for the low- and high-temperature samples were distinguished by the soil temperature of the

Table 1
Summary of methods.

Soil Property	Method
Bulk density ρ_d	Mass loss by oven heating
Total organic carbon	Mass loss by LOI
Sorptivity of water and ethanol S_w and S_e	Tension infiltrometer
Water repellency R	WDPT, Tension infiltrometer
Field saturated hydraulic conductivity K_{fs}	Tension infiltrometer
Soil-water storage	Rainfall simulations

simulated wildfire after Doerr et al. (2004). Low-temperature burns were defined by a soil-surface temperature of 200–250 °C and > 100 °C at 1–2 cm depth; high-temperature burns were defined by a soil-surface temperature of 450–500 °C and > 200 °C at 1–2 cm depth. The fire was simulated using a digital heating gun (Wagner HT3500) with programmed temperature settings. Temperature was monitored at the surface using a laser thermometer and at 1–2 cm depth with a Type K thermocouple. To minimize disturbance to the core, a small hole was drilled into the PVC from the side, and the thermocouple wire was slowly inserted until the exposed wire was at the center point of the core. Soils were heated until temperatures defined above were reached, or after an hour for practical purposes if the desired temperature ranges were not achieved; this happened for all three high-temperature cores due to the difficulty of achieving high temperatures at depth in the soils, which has been recognized in other studies (e.g., DeBano et al., 1977). The average burning time was approximately 40 min.

2.3. Physical soil properties − bulk density and TOC

Soil cores collected in the field were sub-sampled in the laboratory to evaluate ρ_d with depth. The sub-samples were cored out of the larger cores by using thin-walled brass cylinders (5 cm in diameter and 10 cm in height), with one sub-sample taken per field-collected soil core. Each sub-sample was then sub-sectioned with depth every 2.5 cm by extruding the core from the cylinder, resulting in four samples that were placed into soil-moisture cups for oven drying. When surface material was lost due to combustion, the top sub-sample was less than 2.5 cm, but the deeper sub-samples would still be a full 2.5 cm. The upper sampling interval included litter and duff if it was present. Each sub-sample was weighed, placed into an oven at 105 °C for 24 h, then cooled in a desiccator and weighed again (ASTM D7263-09, 2009). If the sub-sample was less than 2.5 cm tall, the height was measured and used to get volume of soil corresponding to the mass of the sub-sample.

TOC was determined by the LOI method, which involves the destruction by heat of all organic matter in the soil or sediment (Schumacher, 2002). Based on the soil texture and sample size after extrusion, the LOI method was conducted using an exposure time of two hours at 550 °C (Heiri et al., 2001).

2.4. Water drop penetration time test

An initial estimate of water repellency persistence was obtained using the WDPT method (Doerr et al., 2004). The WDPT method was repeated five times on different areas of the soil surface of the intact cores to determine the soil's repellency rating (Table 2), using the median time as the final WDPT. The WDPT measurements were discontinued after 3600 s in the interest of time and because convective rain storms are typically less than 1 h in duration.

2.5. Tension infiltrometer

The Decagon Model S Mini Disk Infiltrometer was used to estimate cumulative infiltration, infiltration rates, K_{fs}, S_w, S_e, and an index of water repellency R for the soils. K_{fs} (cm s^{-1}) was estimated according to:

$$K_{fs} = \frac{C_1}{A} \tag{1}$$

where C_1 is the coefficient of the second-order polynomial term fitting the curve of the cumulative infiltration versus the square root of time (Zhang, 1997), and A is the value relating van Genuchten parameters based on the specific soil type to the suction rate and radius of the infiltrometer disk (unitless; Decagon Devices, 2014; here A = 3.9099 given an estimate of the soil as a sandy loam based on a sieve analysis as well as a 2.25-cm infiltrometer radius and a suction of −2 cm). S_e and S_w were estimated using the slope of the cumulative infiltration versus the square root of time for the first 300 s of infiltration. The method from Zhang (1997) was chosen over other methods (e.g. Vandervaere et al., 2000) because initial and final soil-water contents were not measured during the tension infiltrometer tests.

Lichner et al. (2007) proposed that R could be estimated using the relative sorptivity of ethanol and water according to:

$$R = 1.95\frac{S_e}{S_w}. \tag{2}$$

Procedures for tension-infiltrometer experiments with ethanol were the same as those used for water. Ethanol infiltrometer experiments were completed on the same cores as the water infiltrometer experiments, at the same location, but after the water infiltration tests, allowing multiple days in between for the core to dry.

Tension infiltrometer experiments can have issues with the contact between the instrument base and the soil surface. Reynolds and Zebchuk (1996) analyzed how different contact materials such as contact sand or Spheriglass No. 2227 glass spheres affect pressure head and water content, concluding that data varied using different contact materials, depending on the thickness, saturated

Table 2
WDPT class increments and corresponding descriptive repellency rating (Doerr et al., 2004).

WDPT classes (sec)	≤5	> 5, 20,40, 60	80–600	> 600–3600	> 3600
Repellency rating	Wettable	Slight	Strong	Severe	Extreme

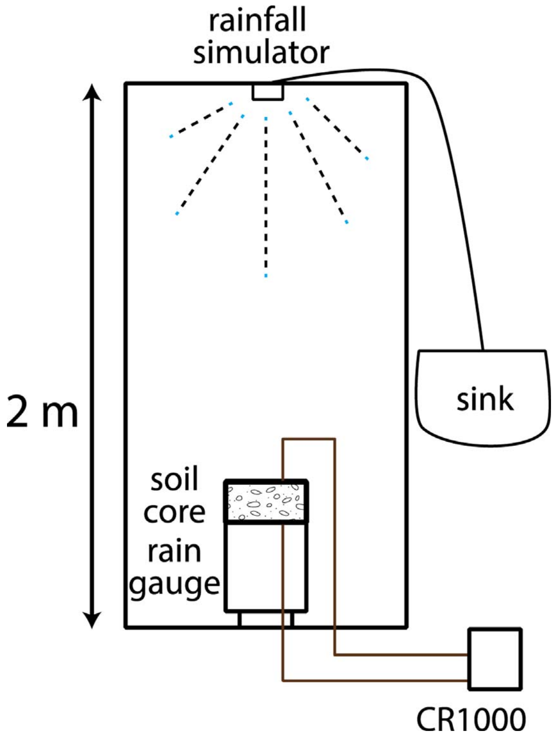

Fig. 2. Rainfall simulator set-up. Core is 10 cm tall and 20 cm in diameter, and sits above a 20-cm diameter Texas Instruments TE525 tipping bucket precipitation gauge attached to a CR1000 data logger.

hydraulic conductivity, and water entry value of the contact material. To eliminate this uncertainty, no contact materials were used and instead a thin layer of surface material was removed to enhance infiltrometer contact. The tension infiltrometer was placed on the soil surface by first removing loose litter and duff material on unburned soil cores. In the high temperature cores, a minimal amount of charred material (1–2 cm) was removed to create a flat surface.

Tension infiltrometer experiments were conducted on each of the three replicates of the unburned control soil as well as for each temperature treatment (i.e. low and high temperature). A suction of −2 cm was used in the infiltrometer tests. Measurements of volume over time were recorded initially every 10 s for the first minute to capture the sorptivity-dominated stage of infiltration. Measurements were then recorded every 30 s until at least 15 mL of water had infiltrated into the soil. Experiment durations varied between 30 min and one hour.

2.6. Rainfall simulation

We simulated precipitation based on a Colorado Front Range storm event with a two-year recurrence interval with 2.5 cm of rainfall over a one-hour duration (UDFCD, 2008). We used a simulator nozzle (Lechler Inc. Full Cone Nozzle Series 490/491 #490.608.1Y.BC) to achieve a consistent rainfall intensity. Each soil core was placed within the rainfall simulator atop a 20-cm diameter Texas Instruments TE525 tipping bucket precipitation gauge (Fig. 2), which measures 0.25-mm rainfall increments per tip, equal to 8.23 mL of water, to record the volume of water passing through the length of the soil core over the one-hour duration. This volume of water was interpreted as outflow, which was related to the amount of water the soil was able to store. Decagon EC-5 soil-moisture probes and Type K temperature thermocouples were inserted horizontally into the soil to measure volumetric water content (VWC) and soil temperature over time. The upper soil-moisture probe and thermocouple were inserted at a depth of approximately 2.5 cm from the surface, while the lower soil-moisture probe and thermocouple were inserted at a depth of approximately 2.5 cm from the bottom of the soil core. The first occurrence of increasing VWC at a sensor, here called breakthrough, was quantified by finding the change in slope in VWC versus time; breakthrough was defined as a positive change in slope and VWC increasing to greater than 10% of the initial VWC.

2.7. Statistical analyses

Non-parametric analyses of variance were conducted to assess the statistical significance of results. Kruskal-Wallis tests were used to test for one-way analysis of variance based on medians (Kruskal and Wallis, 1952). Friedman tests were used for two-way analysis of variance (Friedman, 1937). A significance level (alpha) of 0.05 was used for all tests. Kruskal-Wallis was used to test differences in soil and hydraulic properties across unburned and low- and high- temperature heated samples, and Friedman tests were used to test

Table 3
Change in soil and hydraulic properties from the Boulder Creek Critical Zone intact soil cores associated with burning, relative to one another. Highest values are bolded and lowest in italics for ease of reading. Significance of differences were determined by Kruskal-Wallis tests.

Measurement	Unburned	Low-temperature[a]	High-temperature[b]
ρ_d	No significant change with burning		
TOC	highest	middle	*lowest*
WDPT	middle	highest	*lowest*
Infiltration under tension	middle	*lowest*	**highest**
R	*lowest*	**highest**	middle
K_{fs}	middle	lowest	**highest**
Soil-water storage	No significant change with burning		

[a] Defined by a surface T = 200–250 °C and temperature at 1–2 cm > 100 °C.
[b] Defined by a surface T = 450–500 °C and temperature at 1–2 cm > 200 °C.

differences across soil temperature treatment and with depth in the soil profile.

3. Results and discussion

Here, we outline the change in physical soil properties, soil hydraulic properties, infiltration, and drainage following simulated rainfall as a result of soil burning. Specifically, we describe burning the cores and resultant changes in 1) ρ_d and LOI as a metric of TOC; 2) volumetric soil moisture; 3) water repellency via WDPT and tension infiltrometer measurements; 4) K_{fs}; and 5) drainage of cores following simulated rainfall (Table 1). Overall results are shown in Table 3 in terms of relative changes in properties after burning; details on each of these are described in detail below.

3.1. Wildfire simulations by laboratory burning

Initially, on the unburned soil samples, there was an average of about 2 cm of duff and 3 cm of litter. Litter material consisted of pine needles, leaves, twigs, grass, moss, and pollen cones. When samples were burned to low temperature, between 0–1 cm of duff remained, and most samples had only minor amounts of charred litter (pine needles) left. Soil samples burned to high temperature resulted in no remaining litter or duff layer, which we accommodated for in our depth sampling as noted above by having thinner upper samples. Since the Wagner heat gun blows air using an internal fan, the majority of ash that could have been created during wildfire simulations blew off and did not remain on the soil core. Ash accumulation was therefore not considered in these experiments, although ash can be important for post-wildfire hydrologic response (Burgy and Scott, 1952; Cerdà and Doerr, 2008; Bodí et al., 2012; León et al., 2013).

Low-temperature burned soils reached a temperature of approximately 95 °C at 1–2 cm soil depth after about 35 min of burning, at which point burning was discontinued (Fig. 3). Reaching high temperatures with depth was more challenging; a sharp increase in soil temperature was seen after 50 min during the high-temperature measurements due to complete combustion of surficial organic materials and, potentially, evaporation of water in the early stages resulting in less energy available for heating. Combustion of litter and duff at the surface would occur after approximately 20 min for low-temperature burned soils, and after approximately 3 min for high-temperature burned soils, depending on the surficial materials. The temperatures achieved bracket the soil temperatures at 2.5 cm depth in the heating experiments by DeBano et al. (1979) and are within the range of conditions in the heating experiments by Gabet (2014).

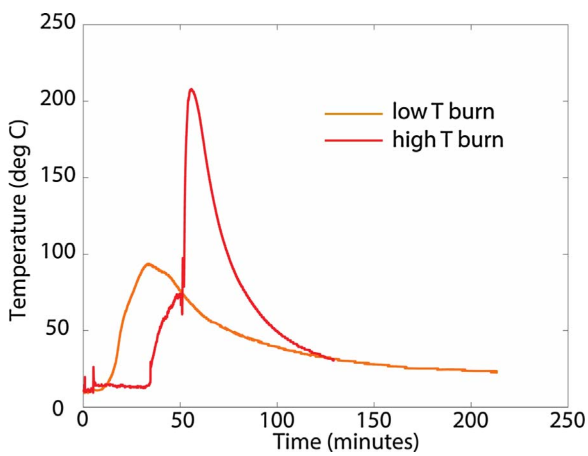

Fig. 3. Temperature measurements collected at 1–2 cm depth from two representative cores during wildfire simulation.

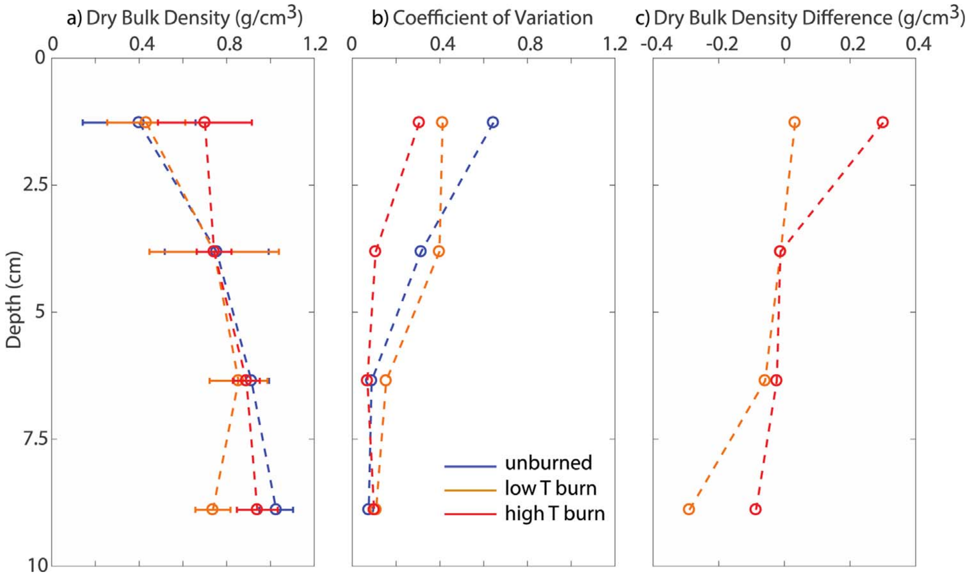

Fig. 4. (a) Mean measured ρ_d (n = 3) with depth for four subsection cores, where error bars indicate +/− one standard deviation for the three replicate samples used for each scenario: unburned control (blue), low-temperature burned (orange), and high-temperature burned (red) soils, (b) the coefficient of variation of ρ_d for each scenario, and (c) the change in mean ρ_d with burning, removing the variation in the control (lowT − unburned; high T − unburned). Significant changes in ρ_d are seen with depth, but not between the control and the burned cores in (a).

3.2. Physical soil properties −ρ_d and TOC

Soil ρ_d varied with depth (Fig. 4a). Average ρ_d (n = 3) increased with depth in unburned soils from approximately 0.4 g/cm^3 at the surface to 1.0 g/cm^3 in the deepest subsection, likely due to an increase in compaction from the collapse of organo-mineral aggregates and an increase in organic concentration near the surface. Low-temperature burned soil replicates exhibited a more variable trend in ρ_d with depth, and average ρ_d was 0.4 g/cm^3 at the surface and 0.7 g/cm^3 in the deepest subsection. At high temperatures, burned soils became homogenized with depth with respect to ρ_d compared to unburned and low-temperature burned soils (Fig. 4a, b). Average ρ_d was 0.7 g/cm^3 at the surface and 0.9 g/cm^3 at the bottom for high-temperature burned soils, although a decrease in the amount of litter and duff led to a smaller sampling volume in the first subsection for some burned soils. In the unburned cores, coefficients of variation in ρ_d were greater near the soil surface due to the variation in the amount of organic litter and duff materials, then decreased with depth. High-temperature burned cores had the lowest coefficients of variation in ρ_d near the soil surface (Fig. 4b), and showed larger changes in ρ_d than low-temperature burning (Fig. 4c), suggesting that high-temperature burning can lead to soil structure degradation (Certini, 2005). Similar increases in near-surface bulk density following wildfire have been shown in other studies (e.g., Giovannini et al., 1988; Andreu et al., 2001; Stoof et al., 2010; Jordán et al., 2011). Moody and Nyman (2013) showed increases in bulk density to a depth of 6 cm on south-facing slopes following the 2010 Fourmile Canyon wildfire in the Colorado Front Range. Despite statistically significant variations in the magnitude of ρ_d and coefficient of variation with depth based on a non-parametric Friedman two-way analysis of variance test (p = 0.0367, p = 0.0498 respectively), there was no statistically significant change in ρ_d magnitude with soil burning between low versus high temperature (p = 0.2881, p = 0.2636, respectively).

We also explored how TOC changed both with depth in the soil and with soil burning. Unburned soil LOI values were 16% on average between 0 and 2.5 cm of soil, and LOI decreased with depth to 6% near the bottom of the soil core (Fig. 5a). Low-temperature burned soils had LOI values near the top of the soil core that averaged 35%, and 9% near the bottom. High-temperature burned soils became homogenized with depth in terms of LOI, with low values throughout (Fig. 5a); average LOI values from the near surface to the bottom of the core were 9% to 7%, respectively, with an increase in LOI between 2.5 and 5 cm depth measuring 11%. Coefficients of variation for TOC were quite variable for the varying subsections regardless of treatment (Fig. 5b). TOC was found to change significantly between temperature treatments, based on a Friedman test (p = 0.0168), and is apparent in Fig. 5c. However, the null hypothesis that the median TOC was the same with changes in depth was not rejected (p = 0.208). TOC changes were inversely proportional to burn temperature, with the greatest change (i.e. reduction in TOC) from the control for high-temperature burned soils (Fig. 5c). The LOI values for low and high-temperature burn samples may be affected by the removal of ash material by the heat gun.

Our results, showing the greatest reduction in organic matter with high-temperature burning, is consistent with prior results for high burn severity by Alauzis et al. (2004) and Hatten and Zabowski (2009), where changes to organic matter depended on burn severity and were concentrated in the O horizon. The unheated LOI average value of 16% is similar to unburned values from the Colorado Front Range reported by Ebel (2012) of 11.2–20.0% and larger than unburned values reported by Moody et al. (2005) of 6.0–7.3% for similar depths below the surface. The high-temperature heated average value off 9% is similar to LOI values at high severity burned sites of 3.1–5.8% reported by Ebel (2012) and Moody et al. (2005) for sites in the Colorado Front Range. Moody and

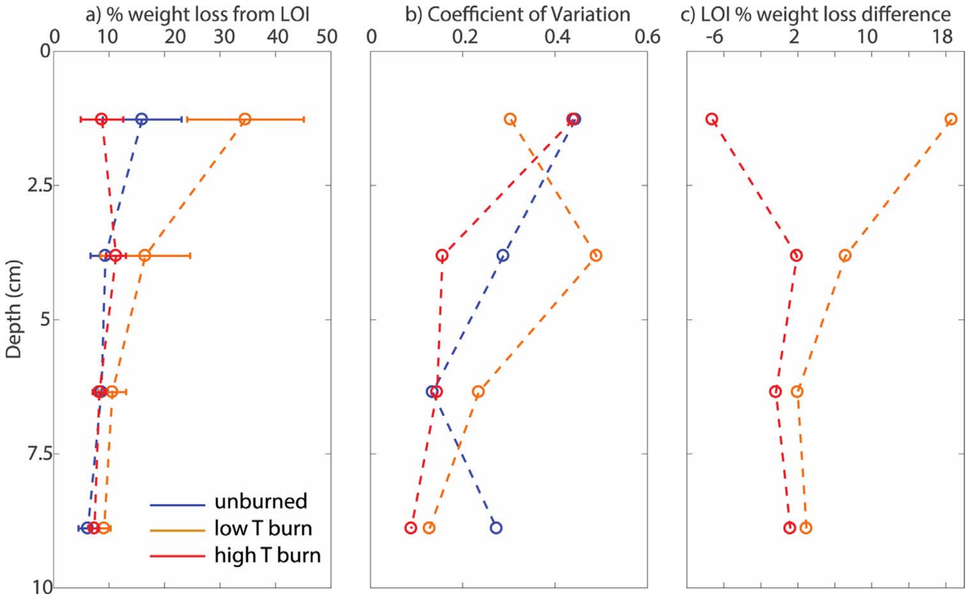

Fig. 5. (a) Mean measured percent weight loss measurements by LOI (n = 3) with depth for four subsection cores, where error bars indicate + / − one standard deviation for the three replicate samples used for each scenario: unburned control (blue), low-temperature burned (orange), and high-temperature burned (red) soils, (b) the coefficient of variation of percent weight loss for each scenario, and (c) the change in percent weight loss with burning, removing the variation in the control (low T − unburned; high T − unburned). TOC was found to vary significantly between treatments in (a).

Nyman (2013) observed the largest LOI decreases in the top 4 cm of soil on south-facing slopes following the 2010 Fourmile Canyon wildfire in the Colorado Front Range. The homogenization of soil organic matter content (i.e. reduction in spatial variability) in the high-temperature burned case is consistent with the work by Cerdà et al. (1995) and Ebel (2012) for high burn severity conditions.

3.3. Water drop penetration time test

Water repellency, based on WDPT, varied by burn temperature with the greatest repellency persistence for low-temperature burned soils and the least repellency persistence for high-temperature burned soils. Based on WDPT class ranges (Table 2), repellency ratings were 1) wettable to strongly repellent for unburned soils, 2) strongly repellent to extremely repellent for low-temperature burned soils, likely due to the condensation of organic hydrophobic coatings, similar to the results shown by Zavala et al. (2009) for low-severity burning, and 3) wettable to slightly repellent for high-temperature burned soils (Table 4). The increase in repellency persistence for the low-temperature burned cores was likely due to the condensation of organic hydrophobic coatings, similar to the results shown by Zavala et al. (2009); reduction and elimination of water repellency with the high-temperature burned cases is likely associated with the volatilization and oxidation of the organic compounds. Changes in WDPT may have occurred below the surface; however, the measurements are only representative of the soil surface. Differences in median WDPT were significant based on Kruskal-Wallis ($p = 0.0001$). Repellency was related to soil temperature, with the highest values for the low-temperature burned case.

Krammes and DeBano (1965) similarly found that heating soils up to 175 °C resulted in little to no change in water repellency,

Table 4
Summary of WDPT test measurements, in seconds.

	Drop 1	Drop 2	Drop 3	Drop 4	Drop 5
Unburned					
1	< 5	< 5	225	80	< 5
2	39	164	12	< 5	5
3	6	< 5	25	64	33
Low-temperature (surface T = 200–250 °C; T at 1–2 cm > 100 °C)					
1	> 3600	> 3600	> 3600	440	> 3600
2	> 3600	2100	570	> 3600	> 3600
3	1990	> 3600	> 3600	> 3600	680
High-temperature (surface T = 450–500 °C; T at 1–2 cm > 200 °C)					
1	35	75	< 5	< 5	< 5
2	< 5	< 5	< 5	< 5	< 5
3	< 5	< 5	< 5	20	< 5

Table 5
Summary table of experimental results averaged over the entire sample depth. The average S_e was used to calculate R for each S_w measurement.

	Tension Infiltrometer Experiments					Rainfall Simulations
Sample Replicates[a]	ρ_d (g/cm^3)	TOC (%)	K_{fs} (cm s^{-1})	S_w (cm s$^{-0.5}$)	Repellency Index, R (−)	Cumulative Outflow (mL)
Unburned						
1	0.61	7.5	1.1×10^{-5}	1.4×10^{-2}	5.0	6.7×10^{2}
2	0.80	13	7.1×10^{-5}	1.3×10^{-2}	5.4	7.5×10^{2}
3	0.91	9.6	4.5×10^{-5}	1.6×10^{-2}	4.4	8.8×10^{2}
Average	0.77	10	3.7×10^{-5}	1.4×10^{-2}	4.9	7.7×10^{2}
Low-temperature (surface T = 200–250 °C; T at 1 2 cm > 100 °C)						
1	0.76	17	2.2×10^{-5}	0.12×10^{-2}	62.7	1.2×10^{3}
2	0.59	23	0.93×10^{-5}	0.51×10^{-2}	14.8	1.8×10^{3}
3	0.85	7.9	2.8×10^{-5}	0.58×10^{-2}	13.0	6.7×10^{2}
Average	0.73	16	2.0×10^{-5}	0.40×10^{-2}	30.2	1.2×10^{3}
High-temperature (surface T = 450–500 °C; T at 1–2 cm > 200 °C)						
1	0.89	9.7	16×10^{-5}	2.0×10^{-2}	10.1	1.5×10^{3}
2	0.71	9.2	11×10^{-5}	12×10^{-2}	1.7	2.0×10^{3}
3	0.86	7.8	14×10^{-5}	3.2×10^{-2}	6.3	1.8×10^{3}
Average	0.82	8.9	14×10^{-5}	5.7×10^{-2}	6.0	1.7×10^{3}

[a] Different soil cores were used for different experiments.

heating between 175 °C and 200 °C considerably increased water repellency, and at higher temperatures (between 280 °C and 400 °C), repellency was destroyed. Others have also shown that repellency disappears in higher temperature ranges (e.g. DeBano, 2000; Doerr et al., 2004; Shakesby et al., 2003) or that with high-severity burns causes major declines in water repellency persistence (e.g., Doerr et al., 2006a,b; Cerdà and Doerr, 2005; Scott and van Wyk, 1990); others have shown the opposite, where high-severity burns show strong repellency just below the surface (e.g., Nyman et al., 2014; Cawson et al., 2016). We note that the variability in times in the unburned soils (less than 5–225 s) likely exists due to the variable presence of naturally occurring water-repellent organic materials prohibiting water infiltration.

3.4. Tension infiltrometer experiments

Soil burning impacted the cumulative infiltration and soil hydraulic properties estimated from the infiltrometer experiments. Low-temperature burned soils infiltrated less water than the unburned control soils, which was expected due to induced water repellency upon burning at lower temperatures. Values of K_{fs} ranged from 1.1×10^{-5} to 7.1×10^{-5} cm s^{-1} for unheated soils, decreased to 0.93×10^{-5}–2.2×10^{-5} cm s^{-1} for low-temperature burned soils, and increased to 11×10^{-5}–16×10^{-5} cm s^{-1} for high-temperature burned soils (Table 5). The mean K_{fs} for high-temperature burned soils was nearly a factor of 7 greater than the K_{fs} for low-temperature burned soils and nearly a factor of 4 greater than unburned soils (Table 5; Fig. 6a). Differences in the median K_{fs} for unburned, low-temperature burned, and high-temperature burned soils were significant based on a Kruskal-Wallis test ($p = 0.0427$). K_{fs} did not change systematically with soil temperature, with the highest K_{fs} values for the high-temperature burned case and the lowest values for the low-temperature burned case.

Estimates of K_{fs} for unburned soils may be lower than expected for a sandy loam soil ($\sim 10^{-4}$; Bagarello and Sgroi, 2007) due to high amounts of organic materials on the soil surface creating natural water repellency, inhibiting the flow of water. The most appropriate wildfire impacted comparison for these K_{fs} estimates was reported by Moody and Ebel (2012) from the 2010 Fourmile Canyon Fire from a high burn severity hillslope. The average K_{fs} value of 2.9×10^{-4} cm s^{-1} from Moody and Ebel (2012) is a factor of ~2–3 times greater than the high-temperature burned results reported here, although Moody and Ebel (2012) also noted infiltration rates of effectively zero for nine of their measurements.

Here, we observed an increase in K_{fs} with high-temperature burning, which is uncommon based upon comparisons with high burn-severity wildfires. Most prior efforts have shown decreases in K_{fs} following wildfire (e.g. Cerdà, 1998; Robichaud, 2000; Neary, 2011; Nyman et al., 2010; Ebel et al., 2012) and substantial decreases in K_{fs} with increasing burn severity (Moody et al., 2016). However, it is important to consider the impact of changes in S_w along with changes in K_{fs} because both gravitational (measured by K_{fs}) and capillary (measured by S_w) contributions to infiltration can be important (e.g. Ebel and Moody, 2017). The mean S_w for high-temperature burned soils was a factor of 14 greater than the S_w for low-temperature burned soils and a factor of 4 greater than unburned soils (Table 5; Fig. 6b). Changes in S_w can result from several effects, such as shifts in pore geometry (Parlange, 1971), soil structure (Shaver et al., 2013), organic material in the litter and duff layers (Czarnes et al., 2000), and water repellency (Hallet et al., 2004). The WDPT times indicate that shifts in water repellency persistence may be responsible for our observed trends in K_{fs} and S_w; R provides additional evidence (Fig. 6d).

The mean R is similar for unburned and high-temperature burned soils, but considerably larger for low-temperature burned soils (Table 5; Fig. 6d)—similar to our WDPT results—with a mean R greater than unburned soil by a factor of 6 and greater than high-temperature burned soil by a factor of 5. The variability in R between samples is much greater in low-temperature burned soil with a standard deviation of 28, while unburned and high-temperature burned soils had lower standard deviations of R of 0.5 and 4.2, respectively. R did not change systematically with increasing soil temperature. The R values indicate that S_w and associated

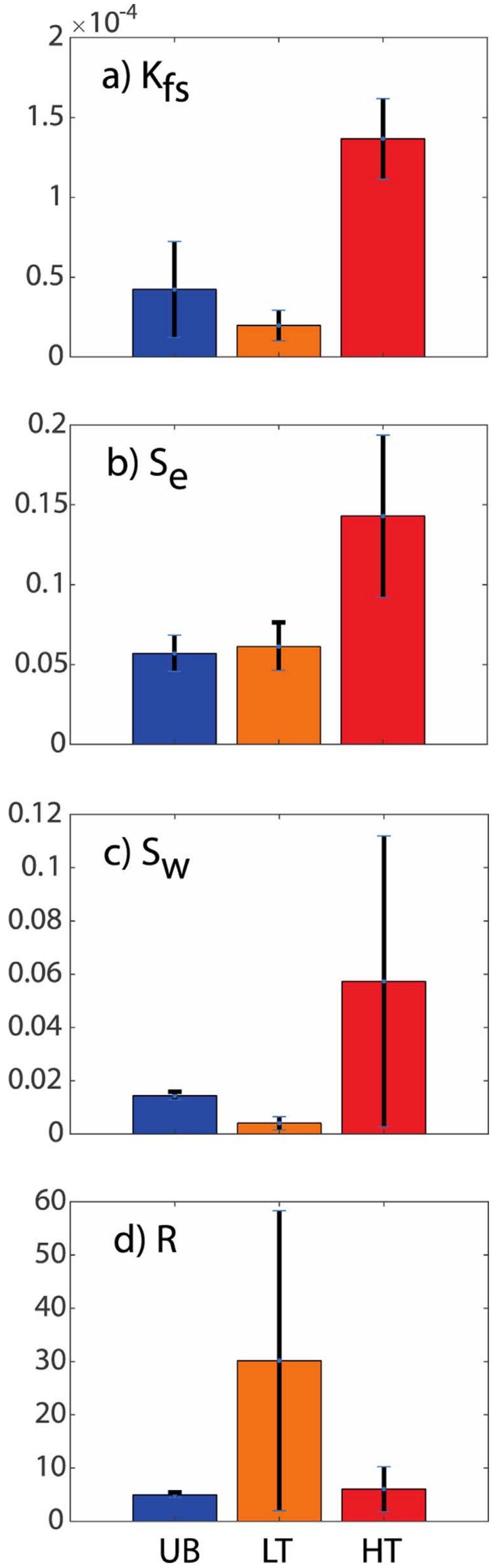

Fig. 6. Comparison of mean (a) field-saturated hydraulic conductivity (K_{fs}), (b) ethanol sorptivity (S_e), (c) water sorptivity (S_w) and water repellency index (R) values with treatment (UB = unburned, LT = low temperature burned, HT = high-temperature burned). Error bars indicate one standard deviation between replicates.

Table 6
Measured VWC during rainfall simulations and changes in VWC during rain event.

		Unburned	Low-temperature	High-temperature
Initial VWC	Top 5 cm	0.12	0.05	0.05
	Bottom 5 cm	0.13	0.08	0.08
Final VWC	Top 5 cm	0.31	0.25	0.30
	Bottom 5 cm	0.30	0.24	0.27
ΔVWC	**Top 5 cm**	**0.19**	**0.20**	**0.25**
	Bottom 5 cm	**0.17**	**0.16**	**0.19**

infiltration rates are lower in the low-temperature burned soils than the unburned soils; burning-enhanced soil-water repellency is apparent in these data and destroyed under high-temperature burning. The reductions in S_w and infiltration rate because of water repellency are consistent with previously reported work by Tillman et al. (1989) and Hallett et al. (2004). The presence of some natural water repellency in unburned soils is also not unusual (DeBano, 1981; Doerr and Moody, 2004; Dekker et al., 2003).

3.5. Rainfall simulations

We achieved average rain intensities of approximately 2.3 cm/hr for all rainfall simulations. For unburned soils, the top 5 cm of soil began with higher initial VWCs than the low- and high-temperature burned soils, which had initially lower VWC as a result of the burning process (Table 6; Fig. 7). High-temperature burned soils saw the first breakthrough of VWC during rainfall in the top soil-moisture sensor after 10 min of raining. Low-temperature burned soils saw a VWC breakthrough in the top soil-moisture sensor at around 12 min. The breakthroughs in unburned soils were delayed due to the presence of litter and duff (organic materials) on the soil surface; the first occurrence of VWC increase occurred after 16 min. The bottom soil moisture sensor in the high-temperature burned and low-temperature burned soil cores saw the first breakthrough of water after 13 min, leading to travel times between

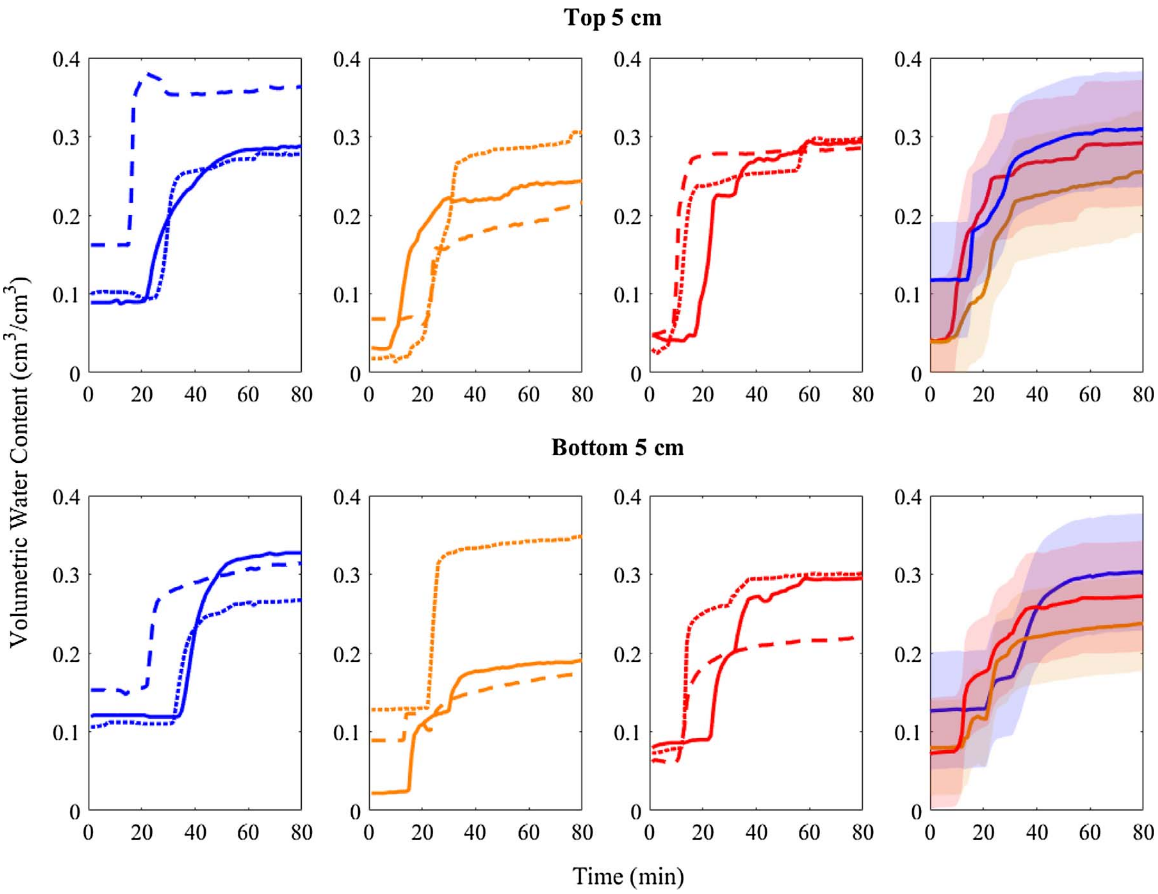

Fig. 7. Breakthrough curves showing VWC over time during rainfall simulations within the upper 5 cm and bottom 5 cm for (a) unheated control, (b) low-temperature burned, and (c) high-temperature burned soils, and (d) the average for each. Shaded regions represent standard deviations. Three replicate samples used for each scenario shown: solid line = first replicate, dotted line = second replicate, dashed line = third replicate.

sensors of 3 and 1 min, respectively. Unburned soils saw breakthrough in the bottom soil moisture sensor later than burned soils, after approximately 23 min of raining, for a travel time of 7 min.

The greatest magnitude of change in soil-water content at 5-cm depth was for the high-temperature burned soils, whereas the unburned and low-temperature burned soils had the same change in soil-water content during rainfall at 5-cm depth within the soil-water content sensor accuracy of ± 0.03 m^3/m^3 (Table 6). High-temperature burned soils also had the greatest change in soil-water content in the bottom 5 cm, whereas the unburned and low-temperature burned soils had the same change in soil-water content at this depth within the soil-water content sensor accuracy. Some ponding during rainfall occurred in all three of the rainfall simulations on the high-temperature burned soils, as well as erosion from raindrop impact, leaving minor amounts of soil at the bottom of the rainfall simulator.

Outflow volumes were measured by the precipitation gauge (Table 5), and were considered related to the soil water storage, with more outflow volume for soils with lower soil-water retention. While high-temperature burned cores had the greatest cumulative outflow volume and unburned soils had the lowest cumulative outflow volume, there is not a significant impact from soil temperature on storage characteristics over the full 10-cm core based on a Kruskal-Wallis test ($p = 0.1479$).

3.6. Implications of results for field settings and limitations of this study

Because of the difficulty in measuring properties in field settings before wildfires, which generally occur unexpectedly, there is a need for controlled laboratory measurements to resolve the effects of wildfire on soil hydraulic properties (Ebel and Moody, 2013). Some implications of the work reported here may be important at the field scale. Low-temperature burned soils had the smallest values of K_{fs} and S_w and the highest values of the water repellency index R and water repellency persistence (Tables 4 and 5; Fig. 6), which would suggest a heightened potential for infiltration-excess overland flow generation in response to rainfall. High-temperature burned soils, in contrast, had the largest values of K_{fs} and S_w and values of R and water repellency persistence similar to unburned soils (Tables 4 and 5 Fig. 6), indicating a lower propensity for infiltration-excess runoff generation although the potential effect of ash in this higher temperature treatment was excluded due to experimental constraints.

The implications based on the data presented here, however, may not align with some field observations as noted previously, due to the simplification of variables for laboratory purposes. First, the role of vegetation in this research was small and strictly on the soil surface, whereas in the field, trees and other vegetation are burned, leading to ash accumulation. While we intended to isolate changes in soil hydraulic properties using laboratory experiments, vegetation could certainly complicate that story in field settings. Second, there may have been some ash intermixing with the shallow soil in post-wildfire simulations given the effects of using the heat gun, which could explain the increases in TOC at shallow depth in low-temperature burned samples. Third, laboratory-scale measurements will always be difficult to extrapolate to the field setting, where the level of heterogeneity is more notable; also, despite best attempts, disturbance to soil during coring or the impact of macropores will affect core-scale results. Scale considerations may be particularly important when considering the spatial connectivity of localized heating effects across hillslopes (e.g. Keizer et al., 2005; Ferreira et al., 2008; Cawson et al., 2013; Langhans et al., 2016; Ebel et al., 2016). An additional limitation of this work is the small number of replicate samples, which is a reflection of the difficulty of extracting intact core from the field. Studies with fewer replicate samples are still important for post-fire meta-analysis studies that synthesize many research efforts with limited sample sizes (e.g. Vieira et al., 2015; Ebel and Moody, 2017), and statistical analyses of small sample sizes have shown to have statistical validity, although results should be evaluated carefully (e.g, de Winter, 2013). Lastly, because burning was performed with a hand-held heat gun, there could also have been inconsistencies across the surface of the soil core, resulting in heterogeneities at the soil surface. This could attribute to variability in WDPT test measurements in low- and high-temperature burned soils between cores.

4. Conclusions

Intact soil cores were collected for laboratory experiments investigating the impacts of wildfire on soil properties and infiltration processes at the Boulder Creek Critical Zone Observatory, in Colorado. Wildfire simulation used a Wagner heat gun, which heated the soil surface to different levels based on temperature and duration. The average ρ_d did not change significantly with changing soil temperature, but it did change significantly with depth in all cores. High-temperature burned soils became homogenized with depth, suggesting the collapse of soil structure. TOC, as measured by LOI, changed significantly with soil temperature treatment. Low-temperature burned soils had some organic materials remaining on the soil surface, whereas all organics were combusted (and blown off) the surface of high-temperature burned soils. Furthermore, the heating of organics was responsible for an increase in water repellency at the surface in low-temperature burned soils, but further burning in the high-temperature scenario destroyed water repellency at the surface, which may have led to the increase in field-saturated hydraulic conductivity with high-temperature burning and more rapid initial VWC breakthrough in simulated rainfall. Soil physical properties of ρ_d and soil organic matter changed in direct proportion to soil temperature, with greater changes for the high temperature cases. Soil-water repellency persistence (WDPT) and the repellency index R, in contrast, peaked at low soil temperatures and declined at high soil temperatures.

Soil-hydraulic properties, such as K_{fs} and S_w, mimicked the changes in soil-water repellency, but did not track with changes in ρ_d or soil organic matter. Trends in TOC and ρ_d did not mimic changes in soil-hydraulic properties, despite some physical linkages between these properties. Linkages were stronger between properties indicating water repellency persistence, WDPT and R, and soil-hydraulic properties K_{fs} and S_w along with infiltration rates.

This research provides insight into how soil hydraulic and physical properties are affected by soil burning in intact soil systems. Laboratory-based experiments, such as the work performed here, could increase the predictive capabilities of forecasting watershed-scale runoff and erosion responses and groundwater recharge post-wildfire. This work suggests that low-temperature burned areas may also provide risk for enhanced runoff generation in the Colorado Front Range. Field work further addressing links between soil temperature and the resulting burn severity with soil hydraulic properties will aid in identifying potential areas of concern, as fire-induced changes affect infiltration, runoff, and erosion potential in this region.

Conflict of interest

There are no known conflicts of interest.

Acknowledgments

The Boulder Creek Critical Zone Observatory is supported by the National Science Foundation (NSF EAR-0724960 at CU-Boulder). Field and laboratory work would not have been possible without the help of Jackie Randell, Colin Barry, Ryan Harmon, Jacob Adamson, and Anny Sainvil. Any use of trade, firm, or product names is for descriptive purposes only and does not imply endorsement by the U.S. Government. Data from this project are available on DSpace, a collection of Colorado digital materials, at https://dspace.library.colostate.edu/handle/11124/170413. Manuscript comments from John Moody, Deborah Martin, and an anonymous reviewer improved the clarity.

Appendix A. Supplementary data

Supplementary data associated with this article can be found, in the online version, at http://dx.doi.org/10.1016/j.ejrh.2017.07.006.

References

ASTMD7263-09 A, 2009. Standard Test Methods for Laboratory Determination of Density (Unit Weight) of Soil Specimens. ASTM Int.. http://compass.astm.org/download/D7263.17262.pdf.

Alauzis, M.V., Mazzarino, M.J., Raffaele, E., Roselli, L., 2004. Wildfires in NW Patagonia: long-term effects on a Nothofagus forest soil. For. Ecol. Manage. 192 (2), 131–142.

Andreu, V., Imeson, A.C., Rubio, J.L., 2001. Temporal changes in soil aggregates and water erosion after a wildfire in a Mediterranean pine forest. Catena 44 (1), 69–84.

Badía, D., Martí, C., 2003a. Plant ash and heat intensity effects on chemical and physical properties of two contrasting soils. Arid L. Res. Manage. 17, 23–41. http://dx.doi.org/10.1080/15324980301595.

Badía, D., Martí, C., 2003b. Effect of simulated fire on organic matter and selected microbiological properties of two contrasting soils. Arid L. Res. Manage. 17, 55–69. http://dx.doi.org/10.1080/15324980301594.

Bagarello, V., Sgroi, A., 2007. Using the simplified falling head technique to detect temporal changes in field-saturated hydraulic conductivity at the surface of a sandy loam soil. Soil Tillage Res. 94 (2), 283–294.

Benavides-Solorio, J., MacDonald, L.H., 2001. Post-fire runoff and erosion from simulated rainfall on small plots, Colorado Front Range. Hydrol. Processes 15 (15), 2931–2952.

Benavides-Solorio, J., MacDonald, L.H., 2005. Measurement and prediction of post-fire erosion at the hillslope scale: Colorado Front Range. Int. J. Wildland Fire 14, 457–474.

Bodí, M.B., Doerr, S.H., Cerdà, A., Mataix-Solera, J., 2012. Hydrological effects of a layer of vegetation ash on underlying wettable and water repellent soil. Geoderma 191, 14–23. http://dx.doi.org/10.1016/j.geoderma.2012.01.006.

Burgy, R.H., Scott, V.H., 1952. Some effects of fire and ash on the infiltration capacity of soils Eos. Trans. Am. Geophys. Union 33 (3), 405–416.

Cancelo-González, Javier, Rial-Rivas, María Ermitas, Barros, Nieves, Díaz-Fierros, Francisco, 2012. Assessment of the impact of soil heating on soil cations using the degree-hours method. Span. J. Soil Sci. 2 (3), 32–44.

Cawson, J.G., Sheridan, G.J., Smith, H.G., Lane, P.N.J., 2013. Effects of fire severity and burn patchiness on hillslope-scale surface runoff: erosion and hydrologic connectivity in a prescribed burn. For. Ecol. Manage. 310, 219–233.

Cawson, J.G., Nyman, P., Smith, H.G., Lane, P.N.J., Sheridan, G.J., 2016. How soil temperatures during prescribed burning affect soil water repellency, infiltration and erosion. Geoderma 278, 12–22. http://dx.doi.org/10.1016/j.geoderma.2016.05.002.

Cerdà, A., Doerr, S.H., 2005. Influence of vegetation recovery on soil hydrology and erodibility following fire: an eleven-year investigation. Int. J. Wildland Fire 14, 423–437.

Cerdà, A., Doerr, S.H., 2008. The effect of ash and needle cover on surface runoff and erosion in the immediate post-fire period. Catena 74 (3), 256–263.

Cerdà, A., Imeson, A.C., Calvo, A., 1995. Fire and aspect induced differences on the erodibility and hydrology of soils at La Costera Valencia, southeast Spain. Catena 24, 289–304.

Cerdà, A., 1998. Changes in overland flow and infiltration after a rangeland fire in a Mediterranean scrubland. Hydrol. Processes 12, 1031–1042.

Certini, G., 2005. Effects of fire on properties of forest soils: a review. Oecologia 143, 1–10. http://dx.doi.org/10.1007/s00442-004-1788-8.

Czarnes, S., Hallett, P.D., Bengough, A.G., Young, I.M., 2000. Root- and microbial-dervied mucilages affect soil structure and water transport. Eur. J. Soil Sci. 51, 435–441. http://dx.doi.org/10.1046/j. 1365–2389.2000.00327.x.

DeBano, L.F., Dunn, P.H., Conrad, C.E., 1977. Fire's Effect on Physical and Chemical Properties of Chaparral Soils. USDA Forest Service General Technical Report WO.

DeBano, L.F., Rice, R.M., Conrad, C.E., 1979. Soil Heating in Chaparral Fires: Effects on Soil Properties, Plant Nutrients, Erosion, and Runoff. USDA Forest Service Research Paper PSW-145. pp. 1–21.

DeBano, L.F., 1981. Water Repellent Soils: A State-of-the-art. General Technical Report PSW-GTR-46 21.

DeBano, L.F., 2000. Water repellency in soils: a historical overview. J. Hydrol. 231–232, 4–32. http://dx.doi.org/10.1016/S0022-1694(00)00180-3.

de Winter, J.C., 2013. Using the Student's *t*-test with extremely small sample sizes Practical Assessment. Res. Eval. 18 (10), 1–12.

Dekker, L.W., DeBano, L.F., Oostindie, K., Elsen, E., Ritsema, C.J., 2003. More than one thousand references related to soil water repellency. Soil Water Repellency: Occurrence, Consequences and Amelioration. Elsevierpp. 315–346.

Devices, Decagon, 2014. Mini Disk Infiltrometer Model S Manual.

Doerr, S.H., Moody, J.A., 2004. Hydrological effects of soil water repellency: on spatial and temporal uncertainties. Hydrol. Processes 18 (4), 829–832.

Doerr, S.H., Blake, W.H., Shakesby, R., Stagnitti, F., Vuurens, S.H., Humphreys, G.S., Wallbrink, P., 2004. Heating effects on water repellency in Australian eucalypt forest soils and their value in estimating wildfire soil temperatures. Int. J. Wildland Fire 13, 157–163. http://dx.doi.org/10.1071/WF03051.

Doerr, S.H., Shakesby, R.A., Blake, W.H., Humphreys, G., Chafer, C., Wallbrink, P.J., 2006a. Effects of differing wildfire severities on soil wettability and implications for hydrological response. J. Hydrol. 319, 295–311.
Doerr, S.H., Shakesby, R.A., Dekker, L.W., Ritsema, C.J., 2006b. Occurrence prediction and hydrological effects of water repellency amongst major soil and land-use types in a humid temperate climate. Eur. J. Soil Sci. 57 (5), 741–754.
Ebel, B.A., Moody, J.A., 2013. Rethinking infiltration in wildfire-affected soils. Hydrol. Processes 27 (10), 1510–1514.
Ebel, B.A., Moody, J.A., 2017. Synthesis of soil-hydraulic properties and infiltration timescales in wildfire-affected soils. Hydrol. Processes 31, 324–340. http://dx.doi.org/10.1002/hyp.10998.
Ebel, B.A., Moody, J.A., Martin, D.A., 2012. Hydrologic conditions controlling runoff generation immediately after wildfire. Water Resour. Res. 48 (3).
Ebel, B.A., 2012. Wildfire impacts on soil-water retention in the colorado front range, United States. Water Resour. Res. 48 (12).
Ebel, B.A., Rengers, F.K., Tucker, G.E., 2016. Observed and simulated hydrologic response for a first-order catchment during extreme rainfall 3 years after wildfire disturbance. Water Resour. Res. 52, 9367–9389. http://dx.doi.org/10.1002/2016WR019110.
Fernández, I., Cabaneiro, A., Carballas, T., 1997. Organic matter changes immediately after a wildfire in an Atlantic forest soils and comparison with laboratory soil heating. Soil Biol. Biochem. 29, 1–11. http://dx.doi.org/10.1016/S0038-0717(96)00289-1.
Ferreira, A.J.D., Coelho, C.D.O., Ritsema, C.J., Boulet, A.K., Keizer, J.J., 2008. Soil and water degradation processes in burned areas: lessons learned from a nested approach. Catena 74, 273–285.
Forgeard, F., Frenot, Y., 1996. Effects of burning on heathland soil chemical properties: an experimental study on the effect of heating and ash deposits. J. Appl. Ecol. 803–811.
Friedman, M., 1937. The use of ranks to avoid the assumption of normality implicit in the analysis of variance. J. Am. Stat. Assoc. 32 (200), 675–701.
Gabet, Emmanuel J., 2014. Fire increases dust production from chaparral soils. Geomorphology 217, 182–192.
Giovannini, G., Lucchesi, S., Giachetti, M., 1988. Effects of heating on some physical and chemical parameters related to soil aggregation and erodibility. Soil Sci. 146 (255–261), 1510–1514. http://dx.doi.org/10.1002/hyp.9696.
Glass, D., Johnson, D., Blank, R., Miller, W., 2008. Factors affecting mineral nitrogen transformations by soil heating: a laboratory-simulated fire study. Soil Sci. 173, 387–400. http://dx.doi.org/10.1097/SS.0b013e318178e6dd.
Hallett, P.D., Nunan, N., Douglas, J.T., Young, I.M., 2004. Millimeter-scale spatial variability in soil water sorptivity. Soil Sci. Soc. Am. J. 68, 352–358.
Hatten, J.A., Zabowski, D., 2009. Changes in soil organic matter pools and carbon mineralization as influenced by fire severity. Soil Sci. Soc. Am. J. 73, 262–273.
Hatten, J.A., Zabowski, D., 2010. Fire severity effects on soil organic matter from a ponderosa pine forest: a laboratory study. Int. J. Wildland Fire 19, 613–623. http://dx.doi.org/10.1071/WF08048.
Heiri, O., Lotter, A.F., Lemcke, G., 2001. Loss on ignition as a method for estimating organic and carbonate content in sediments: reproducibility and comparability of results. J. Paleolimnol. 25, 101–110. http://dx.doi.org/10.1023/A:1008119611481.
Huffman, E.L., MacDonald, L.H., Stednick, J.D., 2001. Strength and persistence of fire-induced soil hydrophobicity under ponderosa and lodgepole pine, Colorado Front Range. Hydrol. Processes 15 (15), 2877–2892.
Jordán, A., Zavala, L.M., Mataix-Solera, J., Nava, A.L., Alanís, N., 2011. Effect of fire severity on water repellency and aggregate stability on Mexican volcanic soils. Catena 84 (3), 136–147.
Kampf, S.K., Brogan, D.J., Schmeer, S., MacDonald, L.H., Nelson, P.A., 2016. How do geomorphic effects of rainfall vary with storm type and spatial scale in a post-fire landscape? Geomorphology 273, 39–51.
Keeley, J.E., 2009. Fire intensity, fire severity and burn severity: a brief review and suggested usage. Int. J. Wildland Fire 18 (1), 116–126.
Keizer, J.J., Coelho, C.O.A., Shakesby, R.A., Domingues, C.S.P., Malvar, M.C., Perez, I.M.B., Matias, M.J.S., Ferreira, A.J.D., 2005. The role of soil water repellency in overland flow generation in pine and eucalypt forest stands in coastal Portugal. Soil Res. 43, 337–349.
Kinoshita, A.M., Chin, A., Simon, G.L., Briles, C., Hogue, T.S., O'Dowd, A.P., Gerlak, A.K., Albornoz, A.U., 2016. Wildfire, water, and society: toward integrative research in. Anthropocene 16, 16–27.
Krammes, J.S., DeBano, L.F., 1965. Soil wettability: a neglected factor in watershed management. Water Resour. Res. 1, 283. http://dx.doi.org/10.1029/WR001i002p00283.
Kruskal, W.H., Wallis, W.A., 1952. Use of ranks in one-criterion variance analysis. J. Am. Stat. Assoc. 47 (260), 583–621. http://dx.doi.org/10.1080/01621459.1952.10483441.
Kunze, M.D., Stednick, J.D., 2006. Streamflow and suspended sediment yield following the 2000 Bobcat ire, Colorado. Hydrol. Processes 20 (8), 1661–1681.
Langhans, C., Lane, P.N., Nyman, P., Noske, P.J., Cawson, J.G., Oono, A., Sheridan, G.J., 2016. Scale-dependency of effective hydraulic conductivity on fire-affected hillslopes. Water Resour. Res. 52 (7), 5041–5055.
León, J., Bodí, M.B., Cerdà, A., Badía, D., 2013. The contrasted response of ash to wetting: the effects of ash type, thickness and rainfall events. Geoderma 209, 143–152.
Lewis, S.A., Wu, J.Q., Robichaud, P.R., 2006. Assessing burn severity and comparing soil water repellency Hayman Fire, Colorado. Hydrol. Processes 20 (1), 1–16.
Lichner, L., Hallett, P.D., Feeney, D., Dugova, O., Sir, M., Tesar, M., 2007. Field measurement of soil water repellency and its impact on water flow under different vegetation. Biologia (Bratisl.) 62 (5), 537–541.
MacDonald, L.H., Huffman, E.L., 2004. Post-fire soil water repellency. Soil Sci. Soc. Am. J. 68 (5), 1729–1734.
Mast, M.A., Murphy, S.F., Clow, D.W., Penn, C.A., Sexstone, G.A., 2016. Water-quality response to a high-elevation wildfire in the Colorado Front Range. Hydrological Processes 30 (12), 1811–1823.
Moody, J.A., Ebel, B.A., 2012. Hyper-dry conditions provide new insights into the cause of extreme floods after wildfire. Catena 93, 58–63.
Moody, J.A., Martin, D.A., 2001. Initial hydrologic and geomorphic response following a wildfire in the Colorado Front Range. Earth Surf. Processes Landforms 26 (10), 1049–1070.
Moody, J.A., Nyman, P., 2013. Variations in Soil Detachment Rates After Wildfire as a Function of Soil Depth, Flow and Root Properties. USGS Scientific Investigations Report 2012-5233Rep. US Geological Survey, Virginia.
Moody, J.A., Smith, J.D., Ragan, B.W., 2005. Critical shear stress for erosion of cohesive soils subjected to temperatures typical of wildfires. J. Geophys. Res.: Earth Surf. 110 (F1). http://dx.doi.org/10.1029/2004JF000141.
Moody, J.A., Kinner, D., Úbeda, X., 2009. Linking hydraulic properties of fire-affected soils to infiltration and water repellency. J. Hydrol. 379, 291–303. http://dx.doi.org/10.1016/j.jhydrol.2009.10.015.
Moody, J.A., Ebel, B.A., Nyman, P., Martin, D.A., Stoof, C., McKinley, R., 2016. Relations between soil hydraulic properties and burn severity. Int. J. Wildland Fire 25 (3), 279–293.
Morris, S.E., Moses, T.A., 1987. Forest fire and the natural soil erosion regime in the Colorado Front Range. Ann. Assoc. Am. Geogr. 77 (2), 245–254.
Murphy, S.F., McCleskey, R.B., Martin, D.A., 2015. The role of precipitation type, intensity, and spatial distribution in source water quality after wildfire. Environ. Res. Lett. 10 (8), 084007.
Natural Resources Conservation Service Soil Survey, 2017. United States Department of Agriculture. Web Soil Survey. (Available online at http://websoilsurvey.nrcs.usda.gov/).
Neary, D.G., 2011. Impacts of Wildfire Severity on Hydraulic Conductivity in Forest, Woodland, and Grassland Soils. Hydraulic Conductivity − Issues, Determination and Applications. In: Elango, Prof. Lakshmanan (Ed.), (ISBN: 978-953-307-288-3, InTech.).
Nyman, P., Sheridan, G., Lane, P.N.J., 2010. Synergistic effects of water repellency and macropore flow on the hydraulic conductivity of a burned forest soil, south-east Australia. Hydrol. Processes 24, 2871–2887. http://dx.doi.org/10.1002/hyp.7701.
Nyman, P., Sheridan, G.J., Smith, H.G., Lane, P.N.J., 2014. Modeling the effects of surface storage, macropore flow and water repellency on infiltration after wildfire. J. Hydrol. 513 (0), 301–313. http://dx.doi.org/10.1016/j.jhydrol.2014.02.044.
Parlange, J.-Y., 1971. Theory of water movement in soils.: 1. One-dimensional absorption. Soil Sci. 111, 134–137. http://dx.doi.org/10.1097/00010694-197102000-00010.
Reynolds, W.D., Zebchuk, W.D., 1996. Use of contact material in tension infiltrometer measurements. Soil Technol. 9, 141–159.

Reynolds, W.D., Elrick, D.E., Topp, G.C., 1983. A re-examination of the constant head well permeameter method for measuring saturated hydraulic conductivity above the water. Table Soil Sci. 136 (4) (p.250).

Robichaud, P.R., 2000. Fire effects on infiltration rates after prescribed fire in Northern Rocky Mountain forests, USA. J. Hydrol. 231–232, 220–229.

Schumacher, B.A., 2002. Methods for the Determination of Total Organic Carbon (TOC) in Soils and Sediments. U.S. Environmental Protection Agency, Washington, DC EPA/600/R-02/069 (NTIS PB2003–100822), 25 p.

Scott, D.F., van Wyk, D.B., 1990. The effects of wildfire on soil wettability and hydrological behaviour of an afforested catchment. J. Hydrol. 121, 239–256.

Shakesby, R.A., Chafer, C.J., Doerr, S.H., Blake, W.H., Wallbrink, P., Humphreys, G.S., Harrington, B.A., 2003. Fire severity, water repellency characteristics and hydrogeomorphological changes following the Christmas 2001 Sydney forest fires. Austr. Geogr. 34, 147–175.

Shaver, T.M., Peterson, G.A., Ahuja, L.R., Westfall, D.G., 2013. Soil sorptivity enhancement with crop residue accumulation in semiarid dryland no-till agroecosystems. Geoderma 192, 254–258. http://dx.doi.org/10.1016/j.geoderma.2012.08.014.

Stoof, C.R., Wesseling, J.G., Ritsema, C.J., 2010. Effects of fire and ash on soil water retention. Geoderma 159, 276–285. http://dx.doi.org/10.1016/j.geoderma.2010.08.002.

Tillman, R.W., Scotter, D.R., Wallis, M.G., Clothier, B.E., 1989. Water repellency and its measurement by using intrinsic sorptivity. Soil Res. 27 (4), 637–644.

UDFCD (Urban Drainage and Flood Control District), 2008. Urban Storm Drainage Criteria Manual: Volume 1 Management, Hydrology, and Hydraulics. UDFCD (Urban Drainage andFlood Control District), Denver, CO (386 p.).

Vandervaere, J.P., Vauclin, M., Elrick, D.E., 2000. Transient flow from tension infiltrometers I. The two-parameter equation. Soil Sci. Soc. Am. J. 64 (4), 1263–1272.

Veblen, T.T., Lorenz, D.C., 1986. Anthropogenic disturbance and recovery patterns in montane forests, Colorado Front Range. Phys. Geogr. 7, 1–24.

Vieira, D.C.S., Fernández, C., Vega, J.A., Keizer, J.J., 2015. Does soil burn severity affect the post-fire runoff and interrill erosion response? A review based on meta-analysis of field rainfall simulation data. J. Hydrol. 523, 452–464. http://dx.doi.org/10.1016/j.jhydrol.2015.01.071.

Wagenbrenner, J.W., MacDonald, L.H., Rough, D., 2006. Effectiveness of three post-fire rehabilitation treatments in the Colorado Front Range. Hydrol. Processes 20 (14), 2989–3006.

Zavala, L.M., Jordán, A., Gil, J., Bellinfante, N., Pain, C., 2009. Intact ash and charred litter reduces susceptibility to rain splash erosion post-wildfire. Earth Surf. Processes Landforms 34, 361–374.

Zhang, R., 1997. Determination of soil sorptivity and hydraulic conductivity from the disk infiltrometer. Soil Sci. Soc. Am. J. 61 (4), 1024–1030.